

## Dominant Auger Process in Electron-Impact Ionization of Mo Ions<sup>(a)</sup>

Yukap Hahn

*Department of Physics, University of Connecticut, Storrs, Connecticut 06268*  
(Received 13 May 1977)

Total ionization cross sections for the highly stripped Mo ions by high-energy electron impact are estimated, including both the direct ionization of outer-shell electrons and the excitation of inner-shell electrons followed by an Auger emission. For highly stripped ions, the excitation to discrete states predominates and enhances the Auger contribution. For the Mo<sup>24+</sup> ions, the Auger ionization of the *L*-shell electrons dominates over the direct *M*-shell ionization.

I present a theoretical estimate of the electron-impact ionization of highly stripped Mo ions, and explicitly demonstrate the dominance of a two-step process in the case of Mo<sup>24+</sup>. Such an enhancement over the direct ionization may seriously affect the analysis of high-energy electron-ion systems in hot-plasma and astrophysical applications.

The ionization of neutral atomic targets by high-energy electron impact takes place mainly through the excitation of outer-shell electrons directly to continuum states, as the inner-shell electrons are generally much harder to excite. However, for heavier ions with increasing degree of ionization  $Z_I$ , the transition probability  $M_C$  for the bound electrons excited directly to continuum decreases much more rapidly than  $M_D$  for the excitation to the allowed discrete states.<sup>1</sup> Therefore, as  $Z_I$  increases, the two-step ionization process becomes important, in which an inner-shell electron is first collisionally excited, followed by the Auger emission of one of the outer-shell electrons as another electron fills the vacancy created. This Auger ionization (AI) process usually contributes to the total cross section a small but significant amount of the order of 10% or less. However, for the Mo<sup>24+</sup> ion considered explicitly here, the Auger ionization in fact dominates over the direct process. Several critical features of the collision involving highly charged ionic targets are pointed out, which enhance the Auger process (and also the dielectronic recombination.)

The total ionization cross section by electron impact of an ionic target with the core charge  $Z_C$  and  $Z_I$  electrons ionized initially is given by

$$\sigma^I = \sigma^{DI} + \sigma^{AI}, \quad (1)$$

where  $\sigma^{DI}$  is the direct ionization cross section, mainly of the outer-shell electrons, and is defined by<sup>2</sup>

$$\sigma^{DI} = \sum_i \sigma_i^{DI}, \quad (2)$$

where, for a given initial state  $i$ , one has

$$\sigma_i^{DI} \approx \frac{8\pi}{p_i^2} N_i M_C D_C \ln \left( \frac{q_{\max}}{q_{\min}} \right). \quad (3)$$

In (3),  $N_i$  is the number of bound electrons in the  $i$ th subshell of the initial ion, and  $M_C$  is the sum of average dipole excitation probabilities for the electrons in the initial orbital ( $n_b l_b$ ) to the entire continuum states, defined by

$$M_C = \langle n_b l_b | \hat{\mathbf{r}} \Lambda_C' \hat{\mathbf{r}}' | n_b l_b \rangle,$$

where  $\Lambda_C'$  is the continuum-state projection operator. The factor  $D_C$  is given<sup>2</sup> in the form  $D_C = D_{\text{amp}} D_{\text{pha}} D_{\text{ret}}$  and takes into account the amplitude, phase distortions of the incident and outgoing electron by the screened Coulomb potentials, and also the correction to the dipole approximation used throughout. The  $q_{\max}$  and  $q_{\min}$  are the usual momentum-transfer cutoffs employed in the Bethe approximation,<sup>3</sup> and we have used the forms<sup>2</sup>  $q_{\max} = [\Delta + (p_i - \sqrt{\Delta})\sqrt{-e_b}] / p_i$  and  $q_{\min} = p_i - p_f$ , which improve the threshold behavior.  $\Delta$  is the average energy transfer.

The Auger ionization cross section  $\sigma^{AI}$  is defined in a similar way as

$$\sigma^{AI} = \sum_i \sigma_i^{AI}, \quad (4)$$

with

$$\sigma_i^{AI} \approx \alpha_i \sigma_i^{DE}. \quad (5)$$

In (5),  $\sigma^{DE}$  is the direct excitation cross section for an inner-shell electron of the initial configuration, raised to an intermediate resonant state, with a creation of an inner-shell vacancy. It is defined by

$$\sigma_i^{DE} \approx \frac{8\pi}{p_i^2} N_i M_D D_D \ln \left( \frac{q_{\max}}{q_{\min}} \right). \quad (6)$$

The subsequent decay of this vacancy by an electron emission is described by the factor  $\alpha_i$ . The quantity  $M_D$  in (6) denotes the sum of the average

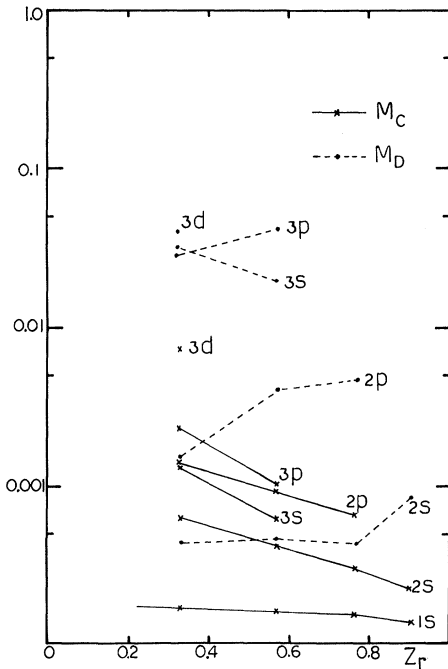


FIG. 1. Average dipole transition probabilities for electrons in the  $(n_b l_b)$  orbital of Mo ions to all the allowed discrete states,  $M_D$ , and to all the continuum states,  $M_C$ .

dipole excitation probabilities to all the allowed discrete states, excluding the continuum and those orbitals which are already occupied. Thus we have

$$M_D = \sum_n' |\langle n_b l_b | \vec{r} | \psi_n \rangle|^2 = \langle n_b l_b | \vec{r} \Lambda_D' \vec{r}' | n_b l_b \rangle.$$

They are related by

$$\Lambda_D' + \Lambda_C' + \Lambda_O' = \delta,$$

where  $\Lambda_O'$  is the projection onto the occupied orbitals. Both  $M_C$  and  $M_D$  are estimated for each initial state using a simple semiclassical approximation<sup>4</sup> for the  $\Lambda$  and a single-particle model<sup>5</sup> for both the initial states and those states included in  $\Lambda$ . They are crude but are accurate enough for our purpose here. The distortion factors  $D_C$  and  $D_D$  have been tested extensively<sup>2</sup>; they are very important when ions with large  $Z_I$  are involved, often increasing the excitation cross section by a large factor.

The AI cross section (5) describes a two-step process of excitation and decay. It thus contains an additional factor  $\alpha_i$ , the Auger decay rate as obtained from the average fluorescence yield  $\omega_i$  by  $\alpha_i = 1 - \omega_i$ . It takes into account the branching rate of decay of a given intermediate state with a vacancy in the  $i$ th inner shell, which is to be

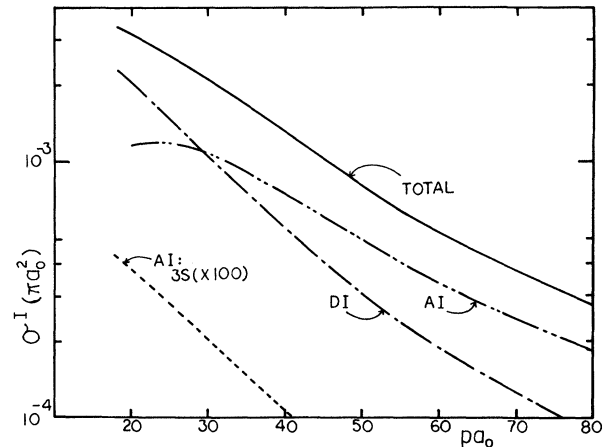


FIG. 2. Total electron impact ionization  $\sigma^I$  for the  $\text{Mo}^{24+}$  ion (solid curve). The direct ionization (DI, dash-dotted line) is compared with the Auger ionization (AI, dash-double-dotted line). The contribution of the 3s electrons is also shown (dashed line).

filled either by a photon emission ( $\omega_i$ ) or by an electron emission ( $\alpha_i$ ). The values for  $\omega$  have been studied most extensively for singly ionized atoms.<sup>6</sup> Since the  $\omega$ 's for the Mo ions are not available, I have made a simple extrapolation of the available  $\omega_K$  for the Ne ions<sup>7,8</sup> and N ions<sup>8</sup> to the  $K$ -,  $L$ -, and  $M$ -shell vacancies.<sup>9</sup>

Obviously,  $\sigma^{\text{AI}}$  can become appreciable only if  $M_D$  for inner-shell electrons becomes large compared to the  $M_C$  for the outer-shell electrons. This is only possible when  $Z_C$  is large and at the same time  $Z_I$  is of a moderate value to have at least the  $L$  shell filled initially. An estimate of  $M_C$  and  $M_D$  is presented in Fig. 1 as functions of  $Z_r \equiv Z_I/Z_C$ . Generally,  $M_D$  increases and  $M_C$  decreases as  $Z_r$  is increased; for  $Z_r \geq 0.5$ ,  $M_D$  completely dominates over  $M_C$ . As noted previously,<sup>1,10</sup> this is probably the most outstanding feature of the highly stripped ions, and strongly influences many of the reactions that involve such ions. The factor  $\alpha_i$  is usually large for small  $Z_r$  and changes slowly as  $Z_r$  increases, provided there are enough outer-shell electrons available for an Auger decay. It decreases very rapidly as  $Z_r$  approaches unity. Therefore, the dominance of  $\sigma^{\text{AI}}$  over  $\sigma^{\text{DI}}$  should be a result of two strongly competing factors  $M_D$  and  $\alpha_i$  versus  $M_C$  and  $\omega_i$ .

For the  $\text{Mo}^{14+}$  and  $\text{Mo}^{32+}$  cases, the AI contribution to the total ionization cross section is estimated to be of the order of 5% and 2%, respectively. On the other hand, in the  $\text{Mo}^{24+}$  case, the  $L$ -shell excitation probability  $M_D$  becomes comparable to the  $M$ -shell ionization probability  $M_C$ ,

so that  $\sigma^{\text{AI}}$  becomes comparable to  $\sigma^{\text{DI}}$  at relatively low energies. The estimated cross sections are plotted in Fig. 2. It shows the dominance of  $\sigma^{\text{AI}}$  for the incident kinetic energy of approximately 12 keV and higher,  $pa_0 \gtrsim 30$ . The energy parameters used in the evaluation of (3) and (5) are generated by the single-particle model<sup>5</sup>;  $\Delta_{3s} = 96.5$  Ry and  $\Delta_{3p} = 92.1$  Ry for the DI, and  $\Delta_{2s} = 180$  Ry =  $\Delta_{2p}$  for the AI excitations. From the extrapolation fit of  $\alpha$  discussed earlier, one obtains  $\alpha_L = 0.90$ , as compared with  $\alpha_L(Z_r = 0) = 0.97$ . The AI contribution comes mainly from the  $2p$  excitation followed by the Auger emission, while the  $2s$  excitation contributes about 4% to the total AI. The contribution of the  $3s$  electrons to the AI by excitations to states just below the ionization threshold is also estimated to be about 3% and less. For the DI cross section, the  $3p$  ionization dominates over the  $3s$  electrons by approximately 5 to 1.

In summary, I have shown that, for reactions involving highly stripped ions,  $\sigma^{\text{DI}}$  alone can often lead to a gross underestimate of the impact ionization cross section. The relative magnitude of  $M_C$  (outer shell) and  $M_D$  (inner shell) is important, but not sufficient to make the AI process dominant, and the branching ratio  $\alpha_i$  plays an important role which warrants much further study. As

$Z_C$  increases, we expect that the dominance of the AI process will be more prevalent even at fairly low  $Z_r$ .

The calculation presented here is only approximate and requires more extensive studies, but its qualitative conclusions are not expected to be seriously affected by the details, which will be reported elsewhere.<sup>9</sup>

<sup>(a)</sup>Work supported in part by the U. S. Energy Research and Development Administration under Contract No. E11-1-2276.

<sup>1</sup>Y. Hahn and K. M. Watson, Phys. Rev. A **7**, 491 (1973).

<sup>2</sup>Y. Hahn, Phys. Rev. A (to be published).

<sup>3</sup>H. A. Bethe and R. W. Jackiw, *Intermediate Quantum Mechanics* (Benjamin, New York, 1968).

<sup>4</sup>Y. Hahn and K. M. Watson, Phys. Rev. A **6**, 548 (1972); Y. Hahn, Phys. Rev. A **13**, 1326 (1976).

<sup>5</sup>P. P. Szydluk and A. E. S. Green, Phys. Rev. A **9**, 1885 (1974).

<sup>6</sup>W. Bambynek *et al.*, Rev. Mod. Phys. **44**, 716 (1972).

<sup>7</sup>M. H. Chen and B. Crasemann, Phys. Rev. A **12**, 959 (1975).

<sup>8</sup>C. P. Bhalla, Phys. Rev. A **12**, 122 (1975), and J. Phys. B **8**, 2792 (1975).

<sup>9</sup>Y. Hahn, to be published.

<sup>10</sup>U. Fano and M. Inokuti, ANL Report No. ANL-76-80, 1976 (unpublished).

## Steady-State Model of a Flat Laser-Driven Target

F. S. Felber

Naval Research Laboratory, Washington, D. C. 20375

(Received 16 February 1977)

A steady-state model of a plasma slab, accelerated by interaction with laser radiation, determines temperature, velocity, and density profiles and boundaries consistent with laser intensity and wavelength and slab mass and acceleration. Density-profile modification is caused by laser pressure. Plasma flows subsonically into the critical surface, and supersonically out.

In an earlier Letter<sup>1</sup> exact transmission coefficients were calculated for intense light incident on a plasma slab in which ions were frozen. In this paper a steady-state model of a plasma slab, accelerated by its interaction with laser radiation, is treated by one-dimensional (1D) steady-flow hydrodynamic equations in an accelerated frame of reference. The cold unablated fluid, the ablation layer, both classical and flux-limited hot conduction regions, the critical surface, and the underdense blowoff are all considered. A global description determines the temperature, density,

velocity, and boundaries as well. Approximate analytic solutions are given in each of the plasma regions.

The ablation layer, containing a steep density gradient separating cold dense fluid from hot low-density plasma, moves at the front of the thermal wave and is accelerated by the rocket reaction to the ablation. Nevertheless Boris has demonstrated through time-dependent numerical simulations that the temperature profile at the ablation layer is steady in an accelerated reference frame, and provided a simplified analytic model of the steady